

# Towards Open-Ended Visual Recognition with Large Language Model

Qihang Yu    Xiaohui Shen    Liang-Chieh Chen  
ByteDance

## Abstract

Localizing and recognizing objects in the open-ended physical world poses a long-standing challenge within the domain of machine perception. Recent methods have endeavored to address the issue by employing a class-agnostic mask (or box) proposal model, complemented by an open-vocabulary classifier (e.g., CLIP) using pre-extracted text embeddings. However, it is worth noting that these open-vocabulary recognition models still exhibit limitations in practical applications. On one hand, they rely on the provision of class names during testing, where the recognition performance heavily depends on this predefined set of semantic classes by users. On the other hand, when training with multiple datasets, human intervention is required to alleviate the label definition conflict between them. In this paper, we introduce the OmniScient Model (OSM), a novel Large Language Model (LLM) based mask classifier, as a straightforward and effective solution to the aforementioned challenges. Specifically, OSM predicts class labels in a generative manner, thus removing the supply of class names during both training and testing. It also enables cross-dataset training without any human interference, exhibiting robust generalization capabilities due to the world knowledge acquired from the LLM. By combining OSM with an off-the-shelf mask proposal model, we present promising results on various benchmarks, and demonstrate its effectiveness in handling novel concepts. Code/model are available at <https://github.com/bytedance/OmniScient-Model>.

## 1. Introduction

A persistent challenge in the realm of machine perception involves the accurate localization [6, 7, 26, 32, 52] and recognition [19, 31, 40] of objects in real-world settings. While considerable progress has been made on various standard benchmarks [35, 61, 73, 81], existing methods continue to grapple with the complexities of real-life scenarios where novel out-of-training dataset concepts frequently arise. To address this issue and enhance the practical utility of models, a common strategy is to decom-

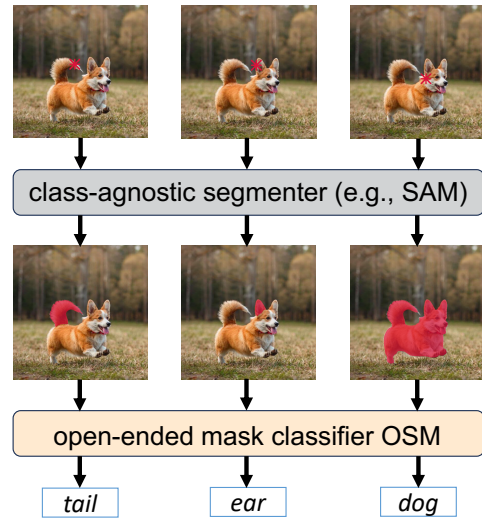


Figure 1. **Illustration of open-ended recognition.** The open-ended recognition task is decomposed into two sub-tasks: class-agnostic mask proposal and open-ended mask classification. To tackle the task, we propose OSM (OmniScient Model), an open-ended recognition model that works hand in hand with an off-the-shelf class-agnostic mask proposal model (e.g., SAM). Unlike existing open-vocabulary recognition models, OSM does not require any user-predefined vocabulary and instead directly predicts the class of each proposal with unconstrained vocabulary in a generative manner. As a result, OSM shows a great generalization ability. For example, we observe **emergent part predictions** such as tail and ear, while OSM has never seen such masks or labels during training (*i.e.*, we do not use any part segmentation datasets during training). Moreover, by obtaining masks from a class-agnostic segmenter, we can take advantage of it and take a wide range of prompt types including point, box, and mask.

pose the problem into two components: class-agnostic mask/box proposal and mask/box classification, as highlighted in previous works [3, 12, 70, 92]. It has been observed that mask/box proposal models, when trained on a dataset such as COCO [47], can still effectively generalize to previously unseen concepts [36, 89]. Additionally, recent advancements, exemplified by Segment Anything Model (SAM) [39], have expanded the training dataset to an exten-

sive scale, encompassing 1.1 billion class-agnostic masks from 11 million images. This has yielded a mask proposal model characterized by robust zero-shot segmentation capabilities, generalizing to novel images and concepts. These developments present a promising avenue toward a solution to the first issue regarding class-agnostic object proposals.

Despite the remarkable achievements in the development of general proposal models, addressing the challenge of classifying novel concepts in real-world scenarios remains an unsolved issue. Many of the existing approaches leverage vision-language models (VLMs), such as CLIP [61] and ALIGN [35], which have been pretrained on extensive Internet datasets and have demonstrated outstanding performance in aligning images and text within a shared embedding space. Specifically, these techniques [21, 25, 46, 74, 77, 84, 89] aim to train open-vocabulary classifiers that rely on the precomputed text embeddings derived from VLMs, as opposed to learning label embeddings directly from the training dataset. The dependency on VLM text embeddings highlights the inherent power and generalization capabilities of VLMs, which, to a certain extent, ensure the classifier’s ability to generalize to novel concepts.

Nevertheless, it is important to acknowledge that while these methods have shown promise, they are still confronted with several challenges that impede their practical application. Firstly, these models typically operate under the assumption that class names are predefined during testing, a condition seldom met in real-life scenarios. Furthermore, when utilizing multiple diverse datasets, complications arise when different label definitions or label space conflicts exist among them. Consequently, many current multi-dataset frameworks address this issue by training on each dataset with an individual decoder or classifier [28, 88, 90], or merge the label space manually [41], adding complexity to the process.

To address these challenges, we introduce OmniScient Model (OSM), a novel generative framework towards open-ended recognition tasks. Instead of training the model to “select” correct classes from a predefined vocabulary, our approach focuses on training it to generate the desired class names. This paradigm shift means that the model no longer requires the prior knowledge of all possible class names provided by users, eliminating the necessity for a well-defined vocabulary during both training and testing phases. Consequently, this approach naturally accommodates the training and testing on datasets with varying label spaces, obviating the need for human intervention to harmonize the differences. Additionally, by building upon a pre-trained Large Language Model (LLM) [14, 67], OSM leverages the implicitly learned world knowledge [33, 63] encoded within the LLM, enhancing its ability to effectively generalize to novel concepts, further bolstering its utility and reliability.

We conduct meticulous experiments to validate the ap-

propriateness of employing a generative model for discriminative tasks. Our investigation includes assessing the generative model’s ability to effectively capture and adapt to the characteristics of a given training dataset and its associated vocabulary. We compare its performance to that of a discriminative model, primarily focusing on classification accuracy. Additionally, we introduce a Mode Query mechanism, which empowers the model to make predictions within a predefined vocabulary (referred to as vocabulary-specific predictions), or to provide open-ended predictions without vocabulary constraints (referred to as vocabulary-agnostic predictions). Finally, we integrate OSM with various off-the-shelf segmentors (*i.e.*, mask proposal models), such as kMaX-DeepLab [83] and SAM [39], and validate its effectiveness across several benchmarks.

## 2. Related Work

**Open-Vocabulary Recognition** Recently, exemplified by CLIP [61] and ALIGN [35], open-vocabulary recognition methods have demonstrated promising outcomes. These methods involve the pre-training of dual-encoder models (for image and text) using contrastive objectives on extensive collections of noisy image-text pairs. This pre-training process yields feature representations that possess cross-model capabilities, showcasing robust performance in zero-shot downstream tasks. Drawing inspiration from these advances, the field of open-vocabulary detection and segmentation has also witnessed remarkable breakthroughs, where class names provided during testing may not have been encountered during the training phase. A majority of these state-of-the-art techniques [21, 25, 46, 74, 84, 89] approach the problem by disentangling it into class-agnostic proposals, along with open-vocabulary proposal classification by leveraging a pre-trained CLIP model. However, despite the impressive accomplishments of these open-vocabulary methods in recognizing unseen classes beyond the training dataset, they hinge on a strong yet brittle assumption that the semantic classes (*i.e.*, vocabulary) are known in advance and remain static, an assumption that can easily be disrupted in practical applications. In parallel with our research efforts, vocabulary-free image classification [16] seeks to address this challenge by dynamically generating vocabularies through processes such as parsing captions [42, 43] or retrieving them from external databases [64]. By contrast, our approach offers a straightforward solution by reformulating the open-ended classification problem as text generation [2, 20, 60, 65], naturally eliminating the need for a user-predefined vocabulary. Furthermore, while our method primarily focuses on object-level recognition, the work presented in [16] concentrates on image-level classification.

**Large Language Models** In recent years, research community has witnessed a remarkable surge in the devel-

opment of Large Language Models (LLMs) [2, 55, 62, 66, 67]. These models have demonstrated impressive emergent capabilities, including in-context learning [2], instruction following [15, 75], and chain-of-thought reasoning [76]. However, a significant limitation of these LLMs is their inherent “blindness” to other modalities, such as visual inputs. More recently, the excitement surrounding multi-modal LLMs has surged, particularly with the introduction of GPT-4V [55]. Pioneering research [1, 5, 43, 48, 49, 72, 91] has illustrated a promising avenue for bridging the gap between language and vision modalities. This approach involves constructing modular models that typically consist of a frozen CLIP vision encoder, a trainable bridging module (e.g., Perceiver Resampler in [1], Q-Former in [43], or a simple linear/MLP layer in [48, 49]), and a frozen LLM. Furthermore, [5, 57, 72, 85, 86] add referring or grounding ability to the multi-modal LLM through taking bounding-box as inputs or outputs. The proposed OSM can be categorized as a modular multi-modal LLMs with referring capability. However, previous endeavors primarily aim to enhance multi-modal LLMs with bounding-box (as bounding-box can be naturally represented in text by referring to its coordinates) for conversation applications, which also require providing vocabulary in the input prompt [72, 85]. Our perspective underscores the value of enabling multi-modal LLMs to recognize *segmentation masks* and serve as standalone tools.

### 3. Method

In this section, we introduce OSM (OmniScient Model), an open-ended recognizer. We commence by detailing how we transform the conventional classification task into a text generation task, aligning with the principles outlined in [2, 60] (Sec. 3.1). Subsequently, we elucidate the construction of OSM, which follows the footsteps of previous modular vision-language models [18, 43, 49, 91] (Sec. 3.2). We also provide a comprehensive overview of our training and evaluation protocols (Sec. 3.3).

#### 3.1. Problem Formulation of Classification

Without loss of generality, we focus our discussion on mask classification. Given an input image  $\mathbf{I} \in \mathbb{R}^{H \times W \times 3}$  and a collection of  $M$  segmentation masks  $\mathbf{M} \in \mathbb{R}^{H \times W \times M}$  (from an off-the-shelf segmenter, e.g., SAM [39]), our objective is to predict a semantic class for each of these masks:

$$\{y_i\}_{i=1}^M = \{(m_i, c_i)\}_{i=1}^M, \quad (1)$$

where  $m_i$  is the  $i$ -th mask from  $\mathbf{M}$  and  $c_i$  is its predicted class, belonging to the set of predefined semantic classes  $C$ , which is assumed to be known during both training and testing phases. In a closed-vocabulary setting, models focus solely on the target classes, implying that the set of predefined semantic classes are identical during both training

and testing (i.e.,  $C_{train} = C_{test}$ , where the subscript denotes the training or testing phase). By contrast, in an open-vocabulary setting, this assumption is relaxed by allowing for the possibility that  $C_{test}$  may include novel categories that were not seen during training (i.e.,  $C_{test} \neq C_{train}$ ). Nevertheless, in both cases, it is essential to have access to the category names of  $C_{train}$  and  $C_{test}$  during both the training and testing stages. As a result, the recognition performance heavily hinges on the careful design of  $C_{train}$  and  $C_{test}$  (called prompt engineering in the literature [25, 84]).

The aforementioned assumption (i.e., the access to  $C_{train}$  and  $C_{test}$ ) plays a pivotal role in contemporary recognition frameworks, whether operating in a closed-vocabulary or open-vocabulary context. These frameworks typically rely on computing similarity logits across semantic class candidates and selecting the candidate with the highest probability as the final prediction. While these methods have demonstrated effectiveness and success across various tasks and benchmarks over the past decades, they are not without critical limitations. Firstly, it is practically impossible to predefine and encompass all potential semantic classes present in the real world. This limitation poses a significant challenge in open-vocabulary recognition since it necessitates the prior definition of novel concepts within the vocabulary. Furthermore, many of these methods are constructed around a handcrafted and meticulously designed label space, with the expectation of covering common concepts that should ideally have unambiguous definitions. However, the manual curation of label spaces may not be scalable, particularly when researchers aim to expand their models to encompass all available datasets from various sources. This process may require labor-intensive tasks such as meticulous manual merging [41] or conducting separate training [28, 88].

To address those challenges, we depart from the conventional approach in visual recognition and propose a novel paradigm named open-ended visual recognition. In this paradigm, we make the bold assumption that the vocabulary  $C$  remains **unknown** during both training and testing. We note that during training we only need to access the target class for each mask, without the need to know the existence of all the other possible classes in  $C$ , which is required for existing methods relying on softmax-based prediction. This shift in perspective is illustrated in Fig. 2 for a holistic comparison of the different paradigms. Rather than selecting a prediction class from a predefined vocabulary, our approach involves directly predicting the class name of the target object. Essentially, this reformulates the recognition task as a text generation problem. Mathematically, we frame open-ended recognition as an endeavor to maximize the conditional likelihood of the class name under a forward

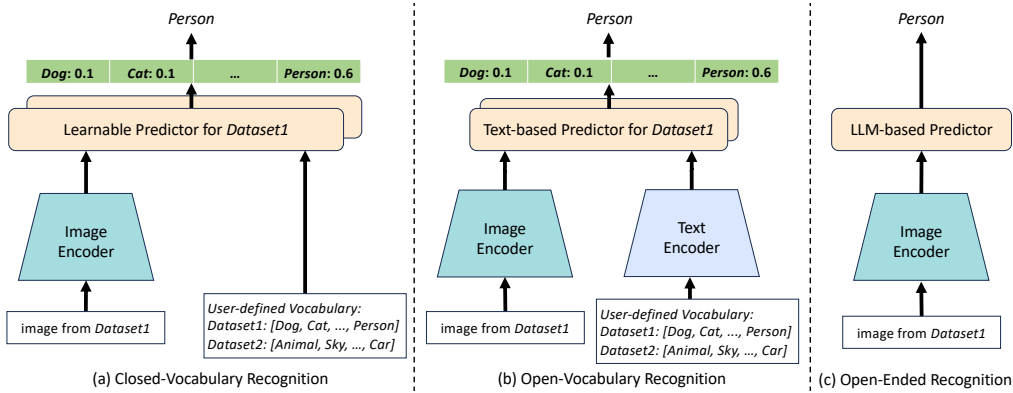


Figure 2. **Comparisons between recognition schemes.** (a) In the closed-vocabulary recognition setting, the sets of semantic classes are fixed during both training and testing. A learnable predictor (*e.g.*,  $1 \times 1$  convolution layer) is used for each training dataset. (b) In the open-vocabulary recognition setting, the sets of semantic classes can be different during training and testing, allowing detection of novel concepts during testing by leveraging a pretrained CLIP backbone. The text-based predictor (*i.e.*, the text embeddings of the predefined set of semantic classes) is different for each dataset. (c) In the open-ended recognition setting, the model directly predicts the class names in a generative manner, removing the need to predefine the semantic classes during training and testing. Additionally, it enables the cross-dataset training in an easier way (*e.g.*, no need to involve humans to resolve the label definition conflicts between datasets).

autoregressive factorization:

$$p(c_i) = \prod_{j=0}^N p(c_{i,j} | c_{i,0}, \dots, c_{i,j-1}), \quad (2)$$

where  $c_{i,j}$  corresponds to the  $j$ -th text token within the class names for  $c_i$ .

### 3.2. Model Architecture

The architectural overview of OSM is presented in Fig. 3. In alignment with the established modular vision-language models [43, 49, 91], OSM comprises three principal components: a frozen CLIP-ViT, a trainable MaskQ-Former, and a frozen Large Language Model (LLM). Our approach incorporates specialized design enhancements aimed at optimizing the model for object-level recognition, which we detail in the following paragraphs:

**High-Resolution Feature Extraction with Frozen CLIP-ViT** A frozen vision transformer backbone, pre-trained in the CLIP style, has become the standard choice in existing multi-modal LLM designs. The appeal of CLIP-ViT lies in its dual advantages: it provides a robust and adaptable feature representation for input images, and its feature space is well-suited for seamless conversion into language tokens, which the LLM can comprehend as inputs.

Nonetheless, the usage of CLIP-ViT, while successful in many multi-modal LLM applications such as image captioning [11, 58] and visual question answering [27, 34], has its limitations. It was originally pre-trained on lower resolutions, typically at resolution  $224 \times 224$ . This lower resolution can hinder its performance, especially when tasked with object-level recognition. Moreover, previous research [84] has observed that a frozen ViT exhibits weak generalization capabilities across varying input resolutions.

Despite the widespread use of frozen ViT backbones in multi-modal LLM models, it is evident that a  $224 \times 224$  input resolution falls short, particularly for object-level recognition. Typical adaptations, such as windowed attention [50] as seen in ViTDet [45], may not be applicable to a completely frozen ViT backbone. To address this limitation, we propose a straightforward strategy to extract more effective features using a frozen ViT at a higher resolution, for example,  $896 \times 896$ . Specifically, we employ a sliding-window feature extraction approach at the input level, where each window size matches that of the ViT’s pre-trained image size. Afterwards, a global positional embedding is added to compensate the missing location information across windows. In our experiments, we will empirically prove that this seemingly simple strategy is surprisingly effective, yielding significantly improved performance in feature extraction from high-resolution inputs. **MaskQ-Former** We employ a visual resampler, such as Q-Former [43] or Perceiver Resampler [1], to bridge the gap between the encoded image features and inputs suitable for the LLM. This visual resampler typically consists of a stack of transformer decoders [69] that transform image tokens into a reduced set of query tokens, which are usually far fewer in number compared to image tokens. However, existing visual resamplers like those used in [1, 43], employ a set of queries that globally attend to image features without considering the segmentation mask priors.

In response to this limitation, we introduce a novel variant called MaskQ-Former. The MaskQ-Former takes a segmentation mask as input and performs masked cross-attention [13], as depicted in Fig. 4. It consists of two sets of learnable queries: mask queries and context queries. The mask queries execute masked cross-attention, restricting their focus to the mask region, while the context queries

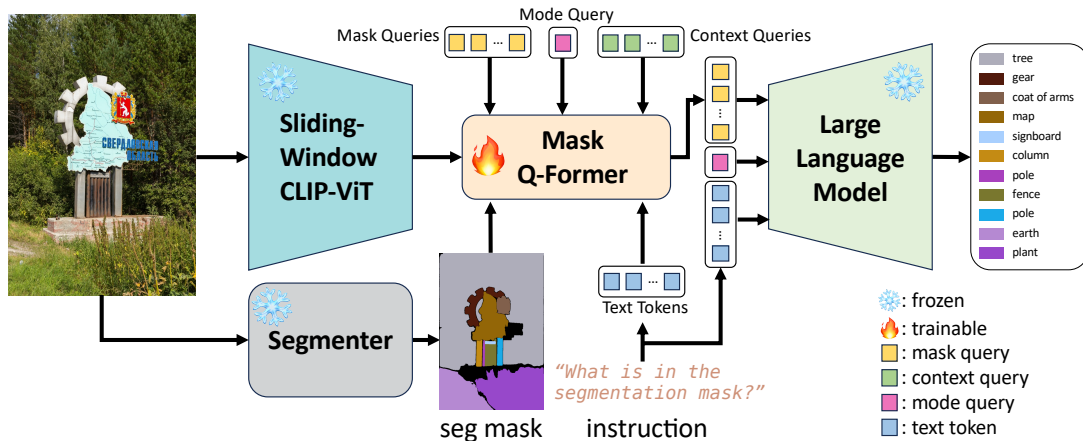


Figure 3. **An overview of the proposed OSM**, consisting of a frozen CLIP-ViT that extracts high-resolution features in a sliding-window manner, a trainable MaskQ-Former that resamples pixel features in a mask-aware manner, and a frozen LLM, which predicts a semantic class for each corresponding mask in a generative manner without a predefined vocabulary. OSM can be combined with any off-the-shelf segmenter, *e.g.*, SAM [39] and kMaX-DeepLab [83]. The proposed MaskQ-Former takes as input (1) Mask Queries, (2) Context Queries, and (3) Mode Query. The Mask Queries focus on the mask regions proposed by the off-the-shelf segmenter, while the Context Queries attend to a broader region derived from the mask. The Mode Query consists of two modes: vocabulary-specific and vocabulary-agnostic, allowing the model to perform with dataset-specific and dataset-agnostic vocabularies, respectively. Note that we have two separate Model Query for MaskQ-Former and LLM respectively, and only the Mask Queries from MaskQ-Former are fed into LLM.

attend to a broader region derived from the mask, such as the bounding box region, to provide complementary contextual information. This contextual information is essential for precise and unbiased recognition [8, 9, 80].

The MaskQ-Former effectively summarizes the mask region while retaining access to essential contextual content. Information exchange between the mask queries and context queries is facilitated through the self-attention layer. Notably, all parameters are shared between the mask and context queries, except for the learnable query initialization, resulting in negligible additional costs. In the end, we retain only the mask queries as inputs to the LLM, ensuring computational efficiency.

**Mode Query** While our primary objective is to enable OSM to perform effectively in an open-ended setting, where it can make predictions without prior knowledge of any vocabulary, we acknowledge the importance of versatility. OSM has the capability to perform accurately when required to align with a specific vocabulary. To achieve this, we introduce Mode Query, consisting of vocabulary-specific and vocabulary-agnostic queries, drawing inspiration from prefix tuning techniques [44]. These queries leverage the strong instruction-following capabilities of the LLM, enhancing the model’s adaptability across diverse scenarios. Concretely, we propose appending a dedicated learnable query for each vocabulary to both the MaskQ-Former and LLM inputs. During training, when utilizing datasets from various sources, the corresponding vocabulary-specific query for each dataset is activated, allowing the model to effectively “memorize” the associ-

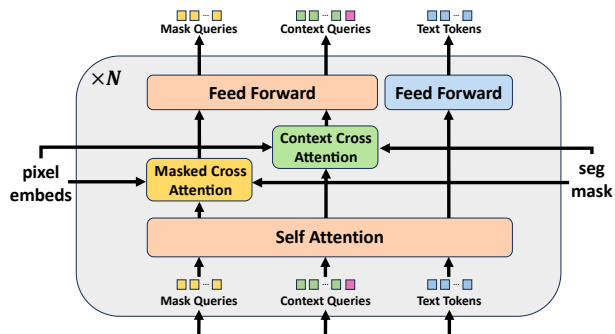


Figure 4. **An overview of MaskQ-Former**. The parameters of Masked Cross Attention layer and Context Cross Attention layer are shared. We append the Mode Query to Context Queries. Moreover, Mask Queries only attend to the mask region in cross-attention layer, while Context Queries may attend to a larger region derived from the mask. All queries/tokens will communicate with each other in the self-attention layer.

ated vocabulary of each dataset, thereby improving alignment during prediction. Additionally, we include a general vocabulary-agnostic query that is activated during training on any dataset to keep the open-ended recognition ability.

This approach provides flexibility during testing. We can activate a vocabulary-specific query to ensure that the model’s predictions align better with the desired vocabulary, or we can activate the vocabulary-agnostic query to facilitate open-ended predictions. This adaptability enhances OSM’s utility across a spectrum of real-world scenarios, making it a versatile tool for a wide range of applications.

### 3.3. Training and Evaluation Protocols

**Datasets** To create a robust training and evaluation framework, we ensemble six publicly available segmentation datasets, encompassing diverse image distributions, domains, and segmentation tasks. These datasets include COCO panoptic segmentation [47], ADE20K panoptic segmentation [87], Cityscapes panoptic segmentation [17], LVIS instance segmentation [29], ADE-847 semantic segmentation [87], and PC-459 semantic segmentation [23].

**Training Protocols** During training, we adopt an instruction tuning approach [15, 49, 75] to seamlessly integrate training with the LLM. For each training iteration, we randomly select an image and its corresponding ground-truth mask from a dataset. We randomly choose an instruction template and insert the actual class name. This approach enables training the model using a straightforward next-token prediction loss without the need for intricate designs. We default to the template *What is in the segmentation mask?* and greedy search decoding for testing.

The choice of training batch size varies across datasets, with batch size 32 for COCO, 64 for LVIS, 16 for ADE-847, 8 for PC-459, 16 for ADE20K, and 8 for Cityscapes, respectively. In each training batch, half of the data activate vocabulary-specific queries corresponding to their respective datasets, while the other half activate vocabulary-agnostic queries. We use AdamW optimizer [37, 53] with learning rate  $4 \times 10^{-5}$  and weight decay 0.05. The learning rate follows a cosine decay schedule. Training continues until the model has processed a total of 6 million masks.

**Evaluation Protocols** Our model is evaluated on the validation set of each dataset, using two types of masks: ground-truth masks or masks produced by an off-the-shelf segmenter. When using ground-truth masks as inputs, we purely assess mask classification accuracy. Specifically, a prediction is considered correct only when the predicted class name **exactly** matches the class name in the ground-truth annotation. To enhance the reliability of this metric, we augment the ground-truth class names with synonyms sourced from [25, 84]. Additionally, we consider plural and singular formats of class names. It is important to note that these synonyms are not used during model training, as they may not always be semantically aligned (*e.g.*, “person”, “man”, and “woman” are synonyms in COCO and LVIS). As a result, we report two metrics: Accuracy (Acc) and Not-in-Vocabulary (NIV), which represent the percentage of predictions correctly match ground-truth classes, or the predictions do not fall into the dataset’s vocabulary, respectively. The metric Acc directly evaluates the model’s classification capacity, while NIV reflects the model’s generalizability or degrees of overfitting to the trained datasets.

Additionally, we consider a more practical application where OSM is connected to an off-the-shelf mask proposal model, such as kMaX-DeepLab [83] or SAM [39]. We

directly evaluate the model’s performance on the established academic benchmarks, including panoptic segmentation and semantic segmentation, using panoptic quality (PQ) [38] and mIoU [23], respectively.

## 4. Experimental Results

In this section, we first provide the settings used for the ablation studies and our final model. We then evaluate OSM with ground-truth masks along with ablation studies in Sec. 4.1, followed by the setting using an off-the-shelf mask proposal model in Sec. 4.2.

**Default Settings for Ablations** Unless otherwise specified, we use the default setting below for ablation studies: We resize both the image and mask during training until the longer side reaches a length of 896 pixels, and then pad the shorter side to match this length. We apply minimal data augmentation, limited to random flipping. The context queries in MaskQ-Former attend to the whole image. We initialize OSM with InstructBLIP [18] pre-trained weight, which uses EVA-ViT-g/224 [24] as vision encoder, and Vicuna-7B [14] as LLM. We use 32 mask queries, 32 context queries, and 1 mode query which is randomly selected between vocab-agnostic query (shared across datasets) and vocab-specific query (one per dataset).

**Settings for Final Models** Based on the findings in the ablation studies (we detail the results later), for our final model, we increase the image resolution to 1120 and the context queries attend to the bounding box region that is  $0.5 \times$  larger than the box-constrained mask region. We also use random scale jittering in the range of [0.5, 1.5].

### 4.1. Mask Classification with Ground-Truth Masks

**Generative Model for Discriminative Tasks** In Tab. 1, we demonstrate that a generative model can effectively capture the training dataset, yielding predictions well-aligned with the training vocabulary. Specifically, as shown in the top few rows of the table (“Single Dataset”), we first train OSM separately on each of the six segmentation datasets, and evaluate its mask classification accuracy using ground-truth masks. Remarkably, the model, although tasked with unrestricted generation of class names, consistently delivers predictions well within the vocabulary of its respective dataset. This is evident by the high percentage of accurate predictions (*i.e.*, high Acc scores) and the very low percentage of predictions falling outside the vocabulary (*i.e.*, low NIV scores), showcasing the generative model’s capacity to operate for a discriminative task.

Next, we explore the more interesting setting, where all six datasets are used for training (“Multiple Datasets” in the table), where OSM still maintains a high accuracy for each individual dataset, even in the presence of potential label conflicts. Specifically, the proposed Mode Query scheme effectively alleviates the label conflicts between datasets,

methods	COCO		LVIS		ADE20K		Cityscapes		A847		PC459		Avg		
	Acc	NIV	Acc	NIV	Acc	NIV	Acc	NIV	Acc	NIV	Acc	NIV	Acc	NIV	
Single Dataset															
COCO Only	85.5	$5.3e^{-5}$	-	-	-	-	-	-	-	-	-	-	-	-	
LVIS Only	-	-	68.3	$2.4e^{-3}$	-	-	-	-	-	-	-	-	-	-	
ADE20K Only	-	-	-	-	82.3	$4.3e^{-4}$	-	-	-	-	-	-	-	-	
Cityscapes Only	-	-	-	-	-	-	79.4	$4.9e^{-4}$	-	-	-	-	-	-	
A847 Only	-	-	-	-	-	-	-	-	76.9	$3.3e^{-3}$	-	-	-	-	
PC459 Only	-	-	-	-	-	-	-	-	-	-	80.9	$6.9e^{-3}$	-	-	
Multiple Datasets															
Learnable Embed	84.3	0.00	67.3	0.00	82.3	0.00	81.0	0.00	76.0	0.00	82.5	0.00	78.9	0.00	
Text Embed	83.4	0.00	65.4	0.00	81.5	0.00	81.6	0.00	75.1	0.00	81.7	0.00	78.1	0.00	
OSM	vocab-agnostic	74.9	11.1	56.8	10.0	80.6	2.31	81.1	0.01	75.6	0.60	77.8	5.69	74.5	4.95
	vocab-specific	84.7	0.10	67.0	0.62	82.1	0.55	81.1	$7.0e^{-5}$	76.4	0.49	80.8	1.90	78.7	0.61
OSM †	vocab-agnostic	79.5	8.75	64.6	8.22	83.8	2.11	88.7	0.01	76.6	0.81	80.6	3.74	79.0	3.94
	vocab-specific	87.0	0.11	72.7	0.94	85.2	0.31	88.6	0.01	78.1	0.49	83.0	0.55	82.4	0.40

Table 1. **Mask classification accuracy across the six segmentation datasets, using ground-truth masks.** Note that OSM (vocab-agnostic) and OSM (vocab-specific) are obtained from the same model and weights, but activate vocabulary-agnostic or vocabulary-specific queries during inference, respectively. NIV: Not-in-Vocabulary. †: Our final model setting.

where the vocabulary-specific queries (“vocab-specific” in the table) better learns the associated vocabulary for each dataset, while the vocabulary-agnostic (“vocab-agnostic”) maintains the open-ended recognition ability (indicated by higher NIV scores). Notably, this achievement is non-trivial and underscores the value of the proposed Mode Query.

Additionally, we establish two discriminative baselines for comparisons. The first one (denoted as “Learnable Embed”) replaces the frozen LLM with six learnable linear layers, each tailored to a specific dataset. The second one (named “Text Embed”) initializes the classification layer with pre-extracted text embeddings and applies it individually to each dataset, approximating the approach presented in [28, 88]. As shown in the table, our generative model OSM performs comparably to the strong baseline “Learnable Embed” on the average (78.7% vs. 78.9% Acc) and outperforms the “Text Embed” baseline. Our findings highlight that the generative model can perform on par with the discriminative models, even in discriminative tasks, underscoring its versatility and effectiveness.

Finally, in the last two rows of the table (denoted as OSM †), using our final model setting (*e.g.*, larger input size) can further significantly improve the performance for both vocabulary-agnostic and vocabulary-specific settings.

**Adaptation to Higher Input Resolution** In contrast to many multi-modal Large Language Models (LLM) approaches that directly employ the frozen CLIP-ViT, we emphasize the critical importance of higher input resolution for achieving accurate object-level recognition. However, we recognize that frozen Vision Transformers (ViTs) often exhibit inferior performance when adapting to larger input resolutions compared to their pre-training resolutions, as documented in [84]. To address this limitation, we introduce

a simple yet highly effective sliding-window approach for obtaining enhanced features from a frozen ViT when processing higher-resolution inputs.

As illustrated in Tab. 2a, our experiments consistently demonstrate performance gains as input resolution increases, particularly from  $224 \times 224$  to  $448 \times 448$ , reflecting an impressive improvement of (+12.8%). This underscores the pivotal role of a larger input resolution in achieving superior object-level recognition performance. The benefits persist until the input resolution reaches  $1120 \times 1120$ , while larger input resolution leads to a performance drop, potentially because each sliding-window fails to capture semantic meaningful feature. Notably, the “Avg NIV” metric remains relatively stable across all experiments, indicating that the performance boost primarily stems from improved mask classification rather than a better overfitting with the respective vocabulary.

**Sliding-Window Stride** We validate our sliding-window design in Tab. 2b, where direct application of the frozen ViT with high-resolution inputs (“Global”) results in significantly inferior performance (−7.2%), consistent with the observations in [84]. Moreover, our findings reveal that employing the sliding-window approach with overlapping windows further enhances results, although the incremental benefit diminishes as the overlap increases. Considering the significant additional computational costs coming from overlapping window, we do not use it in our final setting.

**Effect of Mode Query** It is evident from our experiments that the inclusion of Mode Query plays a pivotal role in the effectiveness of OSM. As demonstrated in Tab. 2c, training OSM across multiple datasets without these queries may result in better generalization capabilities but compromised alignment to specific datasets.

Input Res.	224	448	672	896	1120	1344	1568
Avg Acc	57.3	70.1	75.2	78.7	79.9	76.6	75.9
Avg NIV	0.89	0.84	1.01	0.61	0.74	3.5	3.5

(a) **Input Resolution**

vocab queries	None	Vocab-Agnostic	Vocab-Specific
Avg Acc	74.8	74.5	78.7
Avg NIV	4.45	4.95	0.61

(c) **Mode Query**

Sliding Stride	Global	224	168	112
Avg Acc	71.5	78.7	79.5	79.6
Avg NIV	0.68	0.61	0.59	0.56

(b) **Sliding-Window Stride**

Ratio	Global	0.0×	0.1×	0.2×	0.3×	0.4×	0.5×	0.6×
Avg Acc	78.7	79.5	80.5	80.6	80.9	80.9	81.3	81.0
Avg NIV	0.61	0.51	0.43	0.50	0.62	0.56	0.47	0.50

(d) **Context Enlargement Ratio**

Table 2. **Ablation studies on OSM design choices.** The ablated design choices include (a) image input resolution, (b) the sliding-window stride of the CLIP-ViT backbone to extract high-resolution image features, (c) employment of Mode Query, and (d) the box region size attended by the context queries in MaskQ-Former.

This is evident through a lower ‘‘Avg Acc’’ and a higher ‘‘Avg NIV’’. However, with the integration of the proposed Mode Query, OSM exhibits the ability to operate in both ‘‘closed-ended’’ mode (vocab-specific) and ‘‘open-ended’’ mode (vocab-agnostic). This allows the model to strike a balance between generalization and alignment, preserving both essential capabilities.

**Context is Important for Recognition** We investigate the critical role of context, as detailed in Tab. 2d. Here, ‘‘Global’’ signifies that the context attention may encompass the entire image, whereas ‘‘0.0×’’ refers to a tightly constrained bounding box that encircles the segmentation mask closely. The notation ‘‘ $k\times$ ’’ indicates the expansion of the bounding box by a factor of ‘‘ $k\times$ ’’ on each side. The results in the table underscore the significance of context. Even a tightly defined bounding box offers a noteworthy improvement over global context (+0.8%). Notably, the benefits become more pronounced as we progressively transition to a looser bounding box, with the most substantial gain occurring at ‘‘0.5×’’ (+2.6%) compared to the global context configuration. This underlines the importance of context for accurate recognition, with an optimal balance between tight and loose bounding boxes yielding superior results.

## 4.2. Mask Classification with Off-the-shelf Mask Proposal Model

**Benchmarking with Other Generalists** In addition to evaluating OSM with ground-truth masks, we also provide a practical assessment by integrating OSM with an off-the-shelf mask proposal model. We employ mask proposals generated by kMaX-DeepLab [83] and then apply OSM for classifying these mask proposals. We focus on the comparisons with other generalist segmentation models that are jointly trained with multiple segmentation datasets, similar to our setting. Specifically, we compare with text embedding-based methods like LM-Seg [88] and DaTaSeg [28] across various datasets, including COCO panoptic, ADE20K panoptic and semantic, Cityscapes panoptic, and semantic segmentation. As outlined in Tab. 3, OSM consistently achieves higher Panoptic Quality (PQ) or mean Intersection-over-Union

methods	proposal network backbone	COCO	ADE20K		Cityscapes	
		PQ	PQ	mIoU	PQ	mIoU
Specialist Models (one model per dataset)						
Mask2Former [13]	ResNet50 [31]	51.9	39.7	46.1	62.1	77.5
Mask2Former [13]	Swin-L [50]	57.8	48.1	54.5	66.6	82.9
Generalist Models (one model for all datasets)						
LMSeg [88]	ResNet50 [31]	38.6	35.4	45.2	54.8	80.9
DaTaSeg [28]	ResNet50 [31]	49.0	29.8	48.1	-	-
DaTaSeg [28]	ViTDet-L [45]	53.5	33.4	54.0	-	-
OSM	ResNet50 [31]	53.3	43.8	50.0	59.5	77.0
OSM	ConvNeXt-L [51]	56.1	49.7	55.2	64.7	80.2

Table 3. **Comparison of OSM and other discriminative models.** OSM uses kMaX-DeepLab [83] as the mask proposal model. We mainly compare with the generalist models (LMSeg and DaTaSeg) and list Mask2Former as the specialist model for reference. Note that DaTaSeg [28] uses ADE20K-semantic training data instead of ADE20K-panoptic (thus mark in gray).

(mIoU) scores in comparison to other discriminative methods. Specifically, with ResNet50 proposal model backbone, OSM outperforms LMSeg [88] by +14.7, +8.4, and +4.7 PQ on COCO, ADE20K, Cityscapes respectively. Compared to DaTaSeg [28], OSM also improve the COCO PQ by +4.3, +2.6, the ADE20K mIoU by +1.9, +1.2 for ResNet50 and Large backbone variants, respectively. OSM also shows comparable performance to the specialist model Mask2Former [13].

## 5. Conclusions

In this study, we introduced a novel challenge in the domain of visual recognition, referred to as open-ended visual recognition, and introduced OSM, a generative framework designed to address this challenge. OSM is a mask-aware multi-modal LLM capable of processing segmentation masks as inputs and generating semantic class predictions in a generative manner, without relying on a predefined vocabulary. Our empirical findings demonstrate that this generative model yields promising recognition accuracy and exhibits significant potential for real-world applications, particularly in handling novel concepts that extend beyond predefined vocabularies.

## References

- [1] Jean-Baptiste Alayrac, Jeff Donahue, Pauline Luc, Antoine Miech, Iain Barr, Yana Hasson, Karel Lenc, Arthur Mensch, Katherine Millican, Malcolm Reynolds, et al. Flamingo: a visual language model for few-shot learning. *NeurIPS*, 2022. 3, 4
- [2] Tom Brown, Benjamin Mann, Nick Ryder, Melanie Subbiah, Jared D Kaplan, Prafulla Dhariwal, Arvind Neelakantan, Pranav Shyam, Girish Sastry, Amanda Askell, et al. Language models are few-shot learners. *NeurIPS*, 2020. 2, 3
- [3] Nicolas Carion, Francisco Massa, Gabriel Synnaeve, Nicolas Usunier, Alexander Kirillov, and Sergey Zagoruyko. End-to-end object detection with transformers. In *ECCV*, 2020. 1
- [4] Jun Chen, Deyao Zhu, Xiaoqian Shen, Xiang Li, Zechu Liu, Pengchuan Zhang, Raghuraman Krishnamoorthi, Vikas Chandra, Yunyang Xiong, and Mohamed Elhoseiny. Minigt-v2: large language model as a unified interface for vision-language multi-task learning. *arXiv preprint arXiv:2310.09478*, 2023. 3
- [5] Keqin Chen, Zhao Zhang, Weili Zeng, Richong Zhang, Feng Zhu, and Rui Zhao. Shikra: Unleashing multi-modal llm’s referential dialogue magic. *arXiv preprint arXiv:2306.15195*, 2023. 3
- [6] Liang-Chieh Chen, George Papandreou, Iasonas Kokkinos, Kevin Murphy, and Alan Yuille. Semantic image segmentation with deep convolutional nets and fully connected crfs. In *ICLR*, 2015. 1
- [7] Liang-Chieh Chen, George Papandreou, Iasonas Kokkinos, Kevin Murphy, and Alan L Yuille. Deeplab: Semantic image segmentation with deep convolutional nets, atrous convolution, and fully connected crfs. *TPAMI*, 2017. 1
- [8] Liang-Chieh Chen, George Papandreou, Florian Schroff, and Hartwig Adam. Rethinking atrous convolution for semantic image segmentation. *arXiv preprint arXiv:1706.05587*, 2017. 5
- [9] Liang-Chieh Chen, Yukun Zhu, George Papandreou, Florian Schroff, and Hartwig Adam. Encoder-decoder with atrous separable convolution for semantic image segmentation. In *ECCV*, 2018. 5
- [10] Xianjie Chen, Roozbeh Mottaghi, Xiaobai Liu, Sanja Fidler, Raquel Urtasun, and Alan Yuille. Detect what you can: Detecting and representing objects using holistic models and body parts. In *CVPR*, 2014. 1
- [11] Xinlei Chen, Hao Fang, Tsung-Yi Lin, Ramakrishna Vedantam, Saurabh Gupta, Piotr Dollár, and C Lawrence Zitnick. Microsoft coco captions: Data collection and evaluation server. *arXiv preprint arXiv:1504.00325*, 2015. 4
- [12] Bowen Cheng, Alex Schwing, and Alexander Kirillov. Pixel classification is not all you need for semantic segmentation. *NeurIPS*, 2021. 1
- [13] Bowen Cheng, Ishan Misra, Alexander G Schwing, Alexander Kirillov, and Rohit Girdhar. Masked-attention mask transformer for universal image segmentation. In *CVPR*, 2022. 4, 8
- [14] Wei-Lin Chiang, Zhuohan Li, Zi Lin, Ying Sheng, Zhanghao Wu, Hao Zhang, Lianmin Zheng, Siyuan Zhuang, Yonghao Zhuang, Joseph E. Gonzalez, Ion Stoica, and Eric P. Xing. Vicuna: An open-source chatbot impressing gpt-4 with 90%\* chatgpt quality, 2023. 2, 6
- [15] Hyung Won Chung, Le Hou, Shayne Longpre, Barret Zoph, Yi Tay, William Fedus, Eric Li, Xuezhi Wang, Mostafa Dehghani, Siddhartha Brahma, et al. Scaling instruction-finetuned language models. *arXiv preprint arXiv:2210.11416*, 2022. 3, 6
- [16] Alessandro Conti, Enrico Fini, Massimiliano Mancini, Paolo Rota, Yiming Wang, and Elisa Ricci. Vocabulary-free image classification. *NeurIPS*, 2023. 2
- [17] Marius Cordts, Mohamed Omran, Sebastian Ramos, Timo Rehfeld, Markus Enzweiler, Rodrigo Benenson, Uwe Franke, Stefan Roth, and Bernt Schiele. The cityscapes dataset for semantic urban scene understanding. In *CVPR*, 2016. 6
- [18] Wenliang Dai, Junnan Li, Dongxu Li, Anthony Meng Huat Tiong, Junqi Zhao, Weisheng Wang, Boyang Li, Pascale Fung, and Steven Hoi. Instructblip: Towards general-purpose vision-language models with instruction tuning. *arXiv preprint arXiv:2305.06500*, 2023. 3, 6
- [19] Jia Deng, Wei Dong, Richard Socher, Li-Jia Li, Kai Li, and Li Fei-Fei. Imagenet: A large-scale hierarchical image database. In *CVPR*, 2009. 1
- [20] Jacob Devlin, Ming-Wei Chang, Kenton Lee, and Kristina Toutanova. Bert: Pre-training of deep bidirectional transformers for language understanding. *NAACL*, 2018. 2
- [21] Zheng Ding, Jieke Wang, and Zhuowen Tu. Open-vocabulary panoptic segmentation with maskclip. In *ICML*, 2023. 2, 3
- [22] Alexey Dosovitskiy, Lucas Beyer, Alexander Kolesnikov, Dirk Weissenborn, Xiaohua Zhai, Thomas Unterthiner, Mostafa Dehghani, Matthias Minderer, Georg Heigold, Sylvain Gelly, Jakob Uszkoreit, and Neil Houlsby. An image is worth 16x16 words: Transformers for image recognition at scale. In *ICLR*, 2021. 1
- [23] Mark Everingham, Luc Van Gool, Christopher KI Williams, John Winn, and Andrew Zisserman. The pascal visual object classes (voc) challenge. *IJCV*, 2010. 6
- [24] Yuxin Fang, Wen Wang, Binhui Xie, Quan Sun, Ledell Wu, Xinggang Wang, Tiejun Huang, Xinlong Wang, and Yue Cao. Eva: Exploring the limits of masked visual representation learning at scale. In *CVPR*, 2023. 6
- [25] Golnaz Ghiasi, Xiuye Gu, Yin Cui, and Tsung-Yi Lin. Scaling open-vocabulary image segmentation with image-level labels. In *ECCV*, 2022. 2, 3, 6
- [26] Ross Girshick. Fast r-cnn. In *ICCV*, 2015. 1
- [27] Yash Goyal, Tejas Khot, Douglas Summers-Stay, Dhruv Batra, and Devi Parikh. Making the v in vqa matter: Elevating the role of image understanding in visual question answering. In *CVPR*, 2017. 4
- [28] Xiuye Gu, Yin Cui, Jonathan Huang, Abdullah Rashwan, Xuan Yang, Xingyi Zhou, Golnaz Ghiasi, Weicheng Kuo, Huizhong Chen, Liang-Chieh Chen, and David Ross. Dataset: Taming a universal multi-dataset multi-task segmentation model. *NeurIPS*, 2023. 2, 3, 7, 8
- [29] Agrim Gupta, Piotr Dollar, and Ross Girshick. Lvis: A dataset for large vocabulary instance segmentation. In *CVPR*, 2019. 6

- [30] Ju He, Shuo Yang, Shaokang Yang, Adam Kortylewski, Xiaoding Yuan, Jie-Neng Chen, Shuai Liu, Cheng Yang, Qihang Yu, and Alan Yuille. Partimagenet: A large, high-quality dataset of parts. In *ECCV*, 2022. 1
- [31] Kaiming He, Xiangyu Zhang, Shaoqing Ren, and Jian Sun. Deep residual learning for image recognition. In *CVPR*, 2016. 1, 8
- [32] Kaiming He, Georgia Gkioxari, Piotr Dollár, and Ross Girshick. Mask r-cnn. In *ICCV*, 2017. 1
- [33] Dan Hendrycks, Collin Burns, Steven Basart, Andy Zou, Mantas Mazeika, Dawn Song, and Jacob Steinhardt. Measuring massive multitask language understanding. In *ICLR*, 2021. 2
- [34] Drew A Hudson and Christopher D Manning. Gqa: A new dataset for real-world visual reasoning and compositional question answering. In *CVPR*, 2019. 4
- [35] Chao Jia, Yinfei Yang, Ye Xia, Yi-Ting Chen, Zarana Parekh, Hieu Pham, Quoc Le, Yun-Hsuan Sung, Zhen Li, and Tom Duerig. Scaling up visual and vision-language representation learning with noisy text supervision. In *ICML*, 2021. 1, 2
- [36] Dahun Kim, Tsung-Yi Lin, Anelia Angelova, In So Kweon, and Weicheng Kuo. Learning open-world object proposals without learning to classify. In *ICRA*, 2022. 1
- [37] Diederik P Kingma and Jimmy Ba. Adam: A method for stochastic optimization. In *ICLR*, 2015. 6
- [38] Alexander Kirillov, Kaiming He, Ross Girshick, Carsten Rother, and Piotr Dollár. Panoptic segmentation. In *CVPR*, 2019. 6
- [39] Alexander Kirillov, Eric Mintun, Nikhila Ravi, Hanzi Mao, Chloe Rolland, Laura Gustafson, Tete Xiao, Spencer Whitehead, Alexander C. Berg, Wan-Yen Lo, Piotr Dollár, and Ross Girshick. Segment anything. In *ICCV*, 2023. 1, 2, 3, 5, 6, 4
- [40] Alex Krizhevsky, Ilya Sutskever, and Geoffrey E Hinton. Imagenet classification with deep convolutional neural networks. *NeurIPS*, 2012. 1
- [41] John Lambert, Zhuang Liu, Ozan Sener, James Hays, and Vladlen Koltun. Mseg: A composite dataset for multi-domain semantic segmentation. In *CVPR*, 2020. 2, 3
- [42] Junnan Li, Dongxu Li, Caiming Xiong, and Steven Hoi. Blip: Bootstrapping language-image pre-training for unified vision-language understanding and generation. In *ICML*, 2022. 2
- [43] Junnan Li, Dongxu Li, Silvio Savarese, and Steven Hoi. Blip-2: Bootstrapping language-image pre-training with frozen image encoders and large language models. In *ICML*, 2023. 2, 3, 4
- [44] Xiang Lisa Li and Percy Liang. Prefix-tuning: Optimizing continuous prompts for generation. In *ACL*, 2021. 5
- [45] Yanghao Li, Hanzi Mao, Ross Girshick, and Kaiming He. Exploring plain vision transformer backbones for object detection. In *ECCV*, 2022. 4, 8
- [46] Feng Liang, Bichen Wu, Xiaoliang Dai, Kunpeng Li, Yinan Zhao, Hang Zhang, Peizhao Zhang, Peter Vajda, and Diana Marculescu. Open-vocabulary semantic segmentation with mask-adapted clip. In *CVPR*, 2023. 2, 3
- [47] Tsung-Yi Lin, Michael Maire, Serge Belongie, James Hays, Pietro Perona, Deva Ramanan, Piotr Dollár, and C Lawrence Zitnick. Microsoft coco: Common objects in context. In *ECCV*, 2014. 1, 6
- [48] Haotian Liu, Chunyuan Li, Yuheng Li, and Yong Jae Lee. Improved baselines with visual instruction tuning. *arXiv preprint arXiv:2310.03744*, 2023. 3
- [49] Haotian Liu, Chunyuan Li, Qingyang Wu, and Yong Jae Lee. Visual instruction tuning. *NeurIPS*, 2023. 3, 4, 6
- [50] Ze Liu, Yutong Lin, Yue Cao, Han Hu, Yixuan Wei, Zheng Zhang, Stephen Lin, and Baining Guo. Swin transformer: Hierarchical vision transformer using shifted windows. In *ICCV*, 2021. 4, 8
- [51] Zhuang Liu, Hanzi Mao, Chao-Yuan Wu, Christoph Feichtenhofer, Trevor Darrell, and Saining Xie. A convnet for the 2020s. In *CVPR*, 2022. 8, 1
- [52] Jonathan Long, Evan Shelhamer, and Trevor Darrell. Fully convolutional networks for semantic segmentation. In *CVPR*, 2015. 1
- [53] Ilya Loshchilov and Frank Hutter. Decoupled weight decay regularization. *arXiv preprint arXiv:1711.05101*, 2017. 6
- [54] Thao Nguyen, Samir Yitzhak Gadre, Gabriel Ilharco, Se-woong Oh, and Ludwig Schmidt. Improving multimodal datasets with image captioning. *arXiv preprint arXiv:2307.10350*, 2023. 3
- [55] OpenAI. Gpt-4 technical report. *arXiv preprint arXiv:2303.08774*, 2023. 3, 1
- [56] Jeffrey Ouyang-Zhang, Jang Hyun Cho, Xingyi Zhou, and Philipp Krähenbühl. Nms strikes back. *arXiv preprint arXiv:2212.06137*, 2022. 1
- [57] Zhiliang Peng, Wenhui Wang, Li Dong, Yaru Hao, Shaohan Huang, Shuming Ma, and Furu Wei. Kosmos-2: Grounding multimodal large language models to the world. *arXiv preprint arXiv:2306.14824*, 2023. 3
- [58] Bryan A Plummer, Liwei Wang, Chris M Cervantes, Juan C Caicedo, Julia Hockenmaier, and Svetlana Lazebnik. Flickr30k entities: Collecting region-to-phrase correspondences for richer image-to-sentence models. In *ICCV*, 2015. 4
- [59] Jie Qin, Jie Wu, Pengxiang Yan, Ming Li, Ren Yuxi, Xuefeng Xiao, Yitong Wang, Rui Wang, Shilei Wen, Xin Pan, and Xingang Wang. Freeseq: Unified, universal and open-vocabulary image segmentation. In *CVPR*, 2023. 3
- [60] Alec Radford, Jeffrey Wu, Rewon Child, David Luan, Dario Amodei, and Ilya Sutskever. Language models are unsupervised multitask learners. *OpenAI blog*, 2019. 2, 3
- [61] Alec Radford, Jong Wook Kim, Chris Hallacy, Aditya Ramesh, Gabriel Goh, Sandhini Agarwal, Girish Sastry, Amanda Askell, Pamela Mishkin, Jack Clark, Gretchen Krueger, and Ilya Sutskever. Learning transferable visual models from natural language supervision. In *ICML*, 2021. 1, 2
- [62] Colin Raffel, Noam Shazeer, Adam Roberts, Katherine Lee, Sharan Narang, Michael Matena, Yanqi Zhou, Wei Li, and Peter J Liu. Exploring the limits of transfer learning with a unified text-to-text transformer. *The Journal of Machine Learning Research*, 2020. 3

- [63] Adam Roberts, Colin Raffel, and Noam Shazeer. How much knowledge can you pack into the parameters of a language model? In *EMNLP*, 2020. [2](#)
- [64] Christoph Schuhmann, Romain Beaumont, Richard Vencu, Cade Gordon, Ross Wightman, Mehdi Cherti, Theo Coombes, Aarush Katta, Clayton Mullis, Mitchell Wortsman, et al. Laion-5b: An open large-scale dataset for training next generation image-text models. *NeurIPS*, 2022. [2](#)
- [65] Ilya Sutskever, Oriol Vinyals, and Quoc V Le. Sequence to sequence learning with neural networks. *NeurIPS*, 2014. [2](#)
- [66] Romal Thoppilan, Daniel De Freitas, Jamie Hall, Noam Shazeer, Apoorv Kulshreshtha, Heng-Tze Cheng, Alicia Jin, Taylor Bos, Leslie Baker, Yu Du, et al. Llama: Language models for dialog applications. *arXiv preprint arXiv:2201.08239*, 2022. [3](#)
- [67] Hugo Touvron, Thibaut Lavril, Gautier Izacard, Xavier Martinet, Marie-Anne Lachaux, Timothée Lacroix, Baptiste Rozière, Naman Goyal, Eric Hambro, Faisal Azhar, et al. Llama: Open and efficient foundation language models. *arXiv preprint arXiv:2302.13971*, 2023. [2, 3](#)
- [68] Hugo Touvron, Louis Martin, Kevin Stone, Peter Albert, Amjad Almahairi, Yasmine Babaei, Nikolay Bashlykov, Soumya Batra, Prajjwal Bhargava, Shruiti Bhosale, et al. Llama 2: Open foundation and fine-tuned chat models. *arXiv preprint arXiv:2307.09288*, 2023. [3](#)
- [69] Ashish Vaswani, Noam Shazeer, Niki Parmar, Jakob Uszkoreit, Llion Jones, Aidan N Gomez, Łukasz Kaiser, and Illia Polosukhin. Attention is all you need. *NeurIPS*, 2017. [4](#)
- [70] Huiyu Wang, Yukun Zhu, Hartwig Adam, Alan Yuille, and Liang-Chieh Chen. Max-deeplab: End-to-end panoptic segmentation with mask transformers. In *CVPR*, 2021. [1](#)
- [71] Jiaqi Wang, Pan Zhang, Tao Chu, Yuhang Cao, Yujie Zhou, Tong Wu, Bin Wang, Conghui He, and Dahua Lin. V3det: Vast vocabulary visual detection dataset. In *ICCV*, 2023. [1](#)
- [72] Wenhai Wang, Zhe Chen, Xiaokang Chen, Jiannan Wu, Xizhou Zhu, Gang Zeng, Ping Luo, Tong Lu, Jie Zhou, Yu Qiao, and Jifeng Dai. Visionllm: Large language model is also an open-ended decoder for vision-centric tasks. *NeurIPS*, 2023. [3](#)
- [73] Wenhai Wang, Jifeng Dai, Zhe Chen, Zhenhang Huang, Zhiqi Li, Xizhou Zhu, Xiaowei Hu, Tong Lu, Lewei Lu, Hongsheng Li, Xiaogang Wang, and Yu Qiao. Internimage: Exploring large-scale vision foundation models with deformable convolutions. In *CVPR*, 2023. [1](#)
- [74] Zhenyu Wang, Yali Li, Xi Chen, Ser-Nam Lim, Antonio Torralba, Hengshuang Zhao, and Shengjin Wang. Detecting everything in the open world: Towards universal object detection. In *CVPR*, 2023. [2](#)
- [75] Jason Wei, Maarten Bosma, Vincent Y Zhao, Kelvin Guu, Adams Wei Yu, Brian Lester, Nan Du, Andrew M Dai, and Quoc V Le. Finetuned language models are zero-shot learners. In *ICLR*, 2022. [3, 6](#)
- [76] Jason Wei, Xuezhi Wang, Dale Schuurmans, Maarten Bosma, Fei Xia, Ed Chi, Quoc V Le, and Denny Zhou. Chain-of-thought prompting elicits reasoning in large language models. *NeurIPS*, 2022. [3](#)
- [77] Jiarui Xu, Sifei Liu, Arash Vahdat, Wonmin Byeon, Xiaolong Wang, and Shalini De Mello. Open-vocabulary panoptic segmentation with text-to-image diffusion models. In *CVPR*, 2023. [2, 3, 5](#)
- [78] Mengde Xu, Zheng Zhang, Fangyun Wei, Han Hu, and Xiang Bai. Side adapter network for open-vocabulary semantic segmentation. In *CVPR*, 2023. [3](#)
- [79] Jianwei Yang, Hao Zhang, Feng Li, Xueyan Zou, Chunyuan Li, and Jianfeng Gao. Set-of-mark prompting unleashes extraordinary visual grounding in gpt-4v. *arXiv preprint arXiv:2310.11441*, 2023. [1, 3, 4](#)
- [80] Changqian Yu, Jingbo Wang, Changxin Gao, Gang Yu, Chunhua Shen, and Nong Sang. Context prior for scene segmentation. In *CVPR*, 2020. [5](#)
- [81] Jiahui Yu, Zirui Wang, Vijay Vasudevan, Legg Yeung, Mojtaba Seyedhosseini, and Yonghui Wu. Coca: Contrastive captioners are image-text foundation models. *arXiv preprint arXiv:2205.01917*, 2022. [1](#)
- [82] Qihang Yu, Huiyu Wang, Dahun Kim, Siyuan Qiao, Maxwell Collins, Yukun Zhu, Hartwig Adam, Alan Yuille, and Liang-Chieh Chen. Cmt-deeplab: Clustering mask transformers for panoptic segmentation. In *CVPR*, 2022. [1](#)
- [83] Qihang Yu, Huiyu Wang, Siyuan Qiao, Maxwell Collins, Yukun Zhu, Hartwig Adam, Alan Yuille, and Liang-Chieh Chen. k-means Mask Transformer. In *ECCV*, 2022. [2, 5, 6, 8, 1](#)
- [84] Qihang Yu, Ju He, Xueqing Deng, Xiaohui Shen, and Liang-Chieh Chen. Convolutions die hard: Open-vocabulary segmentation with single frozen convolutional clip. *NeurIPS*, 2023. [2, 3, 4, 6, 7, 5](#)
- [85] Shilong Zhang, Peize Sun, Shoufa Chen, Min Xiao, Wenqi Shao, Wenwei Zhang, Kai Chen, and Ping Luo. Gpt4roi: Instruction tuning large language model on region-of-interest. *arXiv preprint arXiv:2307.03601*, 2023. [3](#)
- [86] Yang Zhao, Zhijie Lin, Daquan Zhou, Zilong Huang, Jiashi Feng, and Bingyi Kang. Bubogpt: Enabling visual grounding in multi-modal llms. *arXiv preprint arXiv:2307.08581*, 2023. [3](#)
- [87] Bolei Zhou, Hang Zhao, Xavier Puig, Sanja Fidler, Adela Barriuso, and Antonio Torralba. Scene parsing through ade20k dataset. In *CVPR*, 2017. [6](#)
- [88] Qiang Zhou, Yuang Liu, Chaohui Yu, Jingliang Li, Zhibin Wang, and Fan Wang. Lmse: Language-guided multi-dataset segmentation. In *ICLR*, 2023. [2, 3, 7, 8](#)
- [89] Xingyi Zhou, Rohit Girdhar, Armand Joulin, Philipp Krähenbühl, and Ishan Misra. Detecting twenty-thousand classes using image-level supervision. In *ECCV*, 2022. [1, 2](#)
- [90] Xingyi Zhou, Vladlen Koltun, and Philipp Krähenbühl. Simple multi-dataset detection. In *CVPR*, 2022. [2](#)
- [91] Deyao Zhu, Jun Chen, Xiaoqian Shen, Xiang Li, and Mohamed Elhoseiny. Minigt-4: Enhancing vision-language understanding with advanced large language models. *arXiv preprint arXiv:2304.10592*, 2023. [3, 4](#)
- [92] Xizhou Zhu, Weijie Su, Lewei Lu, Bin Li, Xiaogang Wang, and Jifeng Dai. Deformable detr: Deformable transformers for end-to-end object detection. In *ICLR*, 2020. [1](#)

# Towards Open-Ended Visual Recognition with Large Language Model

## Supplementary Material

In the supplementary materials, we provide more technical details of OSM. We also include more quantitative results and qualitative results, along with comparisons with GPT-4V [55]. Moreover, we show that OSM can also be easily extended with part-level and box-level datasets, further unleashing the potential of OSM.

**Instruction Template** We summarize the instruction template we used for OSM training in Tab. 4.

**Dilemma between Accuracy and Generalization** We also train OSM under different seen number of masks (*i.e.*, 1, 3, 6, 9 millions respectively), as shown in Fig. 5. Empirically, we consider Acc as a metric to measure how well the model can accurately recognize the object and NIV as a metric to measure the generalization ability. We note that there exists a dilemma between the accuracy and generalization, *i.e.*, when the number of seen masks increases, we notice that the model achieves higher accuracy while inevitably having a higher overfitting to the training vocabulary, and predicts in a more conservative manner. From 6M to 9M, the accuracy improvement majorly comes from the decrease of NIV. We note that how to ensure an accurate object recognition while avoid overfitting to the training vocabulary is an interesting future research problem.

**Incorporating Part- and Box-level Datasets** It is worth noting that OSM seamlessly accommodates part-level and box-level datasets, further enhancing its versatility. To enhance OSM for part-level and box-level recognition (note that OSM already shows emergent part recognition ability as illustrated in Fig. 1, but we believe introducing such datasets could further advance its ability), we introduce PartImageNet [30], Pascal-Part [10], and V3Det [71] datasets into the training data. For part data, we prepend the object name to part name, in case many parts sharing the same names (*e.g.*, in PartImageNet, many different classes may have the same part named *head*). We also remove those class names which are too vague (*e.g.*, *train left side*, *bus upper side* in Pascal-Part). For detection data, we consider the bounding-box as a box-shaped binary mask and thus is easily unified into OSM. Additionally, we augment the panoptic/instance segmentation data (*e.g.*, COCO, LVIS) by randomly converting each segmentation mask into its corresponding bounding box. In cases where a bounding box serves as input, we appropriately adjust the instruction by replacing the term “segmentation mask” with “bounding box.” It’s worth mentioning that we do not include image-level data (*e.g.*, ImageNet) at this stage, as the semantic label could introduce bias when there exist multiple objects yet sharing single label. We demonstrate their effects in Fig. 6, where we use SAM [39] and DETA [56] as the

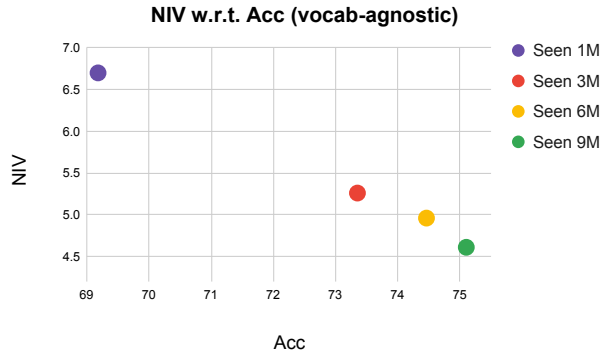


Figure 5. NIV w.r.t. Acc, when number of seen masks varies. The Acc increases as the number of seen masks increases, showing that the model is better trained to fit the target dataset. However, its NIV score becomes much lower, indicating that the model is losing the generalization ability.

proposal model respectively.

**Qualitative Results** We explore the application of OSM on top of SAM [39] and kMaX-DeepLab [83], and provide qualitative results, which are presented in Fig. 7 and Fig. 8 respectively. These results underscore the superiority of OSM in practical scenarios and its potential to demonstrate open-ended recognition with fine-grained masks. When obtaining mask proposals from SAM [39], we use the SAM variant with ViT-H [22] backbone, with points per side 32, IoU threshold 0.95, stability threshold 0.95, and minimum mask size 800. This helps avoid too many small masks that are not recognizable (*e.g.*, super-pixel level masks). When obtaining mask proposals from kMaX-DeepLab [83], we use the one trained on COCO Panoptic dataset with ConvNeXt-L [51] backbone, and we set the “thing” and “stuff” threshold to 0.1 to obtain more mask proposals and feed them into OSM. Afterwards, we apply mask-wise post-processing following [82, 83].

**Comparison against GPT-4V** We provide a qualitative comparison between GPT-4V and OSM. We follow [79] to prompt GPT-4V for mask recognition. Specifically, we highlight the mask boundaries as auxiliary cues in the image, and annotate each mask center with a numeric ID. We feed the prompted image to GPT-4V, along with text prompt “I have labeled a bright numeric ID at the center for each visual object in the image. Please enumerate their names (*i.e.*, semantic class) with one, two, or three words.”. The results are shown in Fig. 9, with first column showing the image after mask prompting and fed to GPT-4V, and

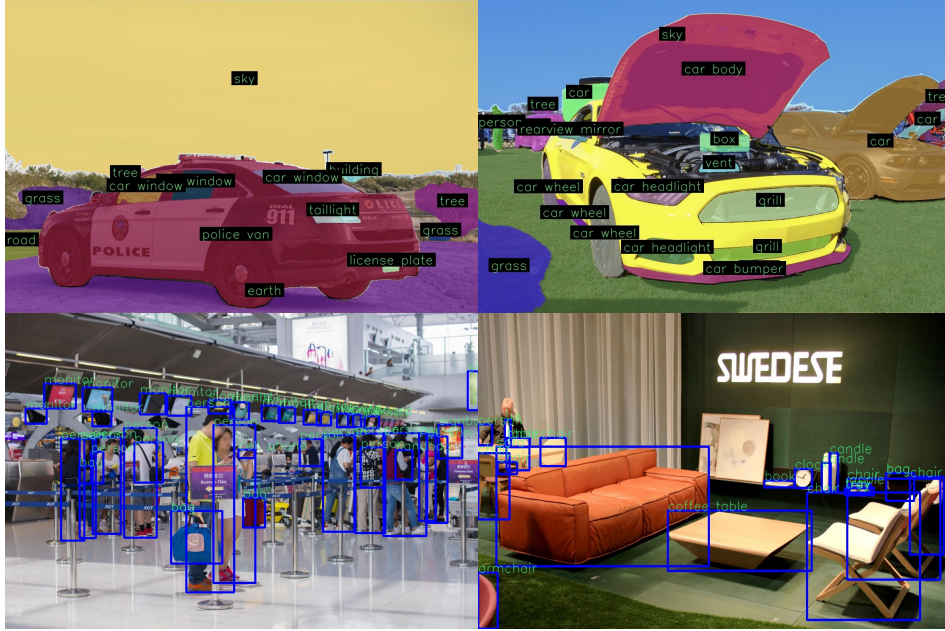


Figure 6. **Extending OSM with part-level and box-level dataset.** We note that the OSM framework is general and we can easily extend it with part-level and box-level data, leading to a stronger performance and more diverse usage. Best viewed zoom in to see predicted class names.

---

1. What is in the segmentation mask? Assistant: {class_name}
2. Describe what is in the segmentation mask. Assistant: {class_name}
3. What does this segmentation mask show? Assistant: {class_name}
4. What is this segmentation mask? Assistant: {class_name}
5. What is the segmentation mask region of the image? Assistant: {class_name}
6. Briefly describe what you perceive in the segmentation mask region. Assistant: {class_name}
7. Please tell the category of what is indicated by the segmentation mask. Assistant: {class_name}
8. What does this segmentation mask segments? Assistant: {class_name}
9. What does this segmentation mask capture? Assistant: {class_name}
10. Answer the name of what is in the segmentation mask region. Assistant: {class_name}
11. What is the semantic class of the area given the segmentation mask? Assistant: {class_name}
12. Can you describe what is in the segmentation mask region? Assistant: {class_name}
13. From the image and segmentation mask provided, tell the category of the indicated region. Assistant: {class_name}
14. Could you use a few words to describe what is in the segmentation mask region? Assistant: {class_name}
15. Given the image and segmentation mask, answer what is in the region. Assistant: {class_name}
16. Tell me what you see in the segmentation mask region. Assistant: {class_name}
17. What can you see in the segmentation mask region? Assistant: {class_name}
18. Let me know what you can perceive in the mask region. Assistant: {class_name}
19. Give me the name of the object in the segmentation mask. Assistant: {class_name}

---

Table 4. **Instruction templates.** We randomly select one instruction template and insert the ground-truth class name during training. Only the first template *What is in the segmentation mask?* is used during testing.

second column for GPT-4V predictions, third column for OSM predictions. We observe that OSM has a more accurate prediction compared to GPT-4V (e.g., in the first row, OSM correctly predicts mask 5 and 11 as *bench* and *fence*, while GPT-4V wrongly predicts them both as *streetlight*),

which is often confused by the context (e.g., in the first row, for the mask 10, GPT-4V predicts *buildings* instead of *mountain*, potentially due to confusion from the buildings below). However, we also note that OSM’s prediction is more conservative compared to GPT-4V, which can pre-





ing the geometric ensemble method, OSM shows superior scores against state-of-the-art open-vocabulary methods, indicating its strong performance. When using the geometric ensemble from another frozen CLIP, OSM still shows a comparable performance with other state-of-the-art methods, such as ODISE [77] and FC-CLIP [84].

**Visualization of NIV Cases** To better understand what are NIV (Not-in-Vocab) cases, we visualize them using ground-truth mask against ground-truth annotation for COCO *val* set and ADE20K *val* set in Fig. 10 and Fig. 11 respectively. We note that with a pre-defined vocabulary, even the ground-truth annotations are usually biased and limited, where annotators have to pick a most similar class in the given vocabulary (*e.g.*, all *monitor* are labeled as *tv* in COCO). The biases could be learnt and inherited in existing closed-vocabulary and open-vocabulary models. However, we observe the OSM can predict a more appropriate class name without limitation of a given vocabulary, demonstrating the necessity and effectiveness of getting rid of a pre-defined vocabulary and pursuing open-ended visual recognition.

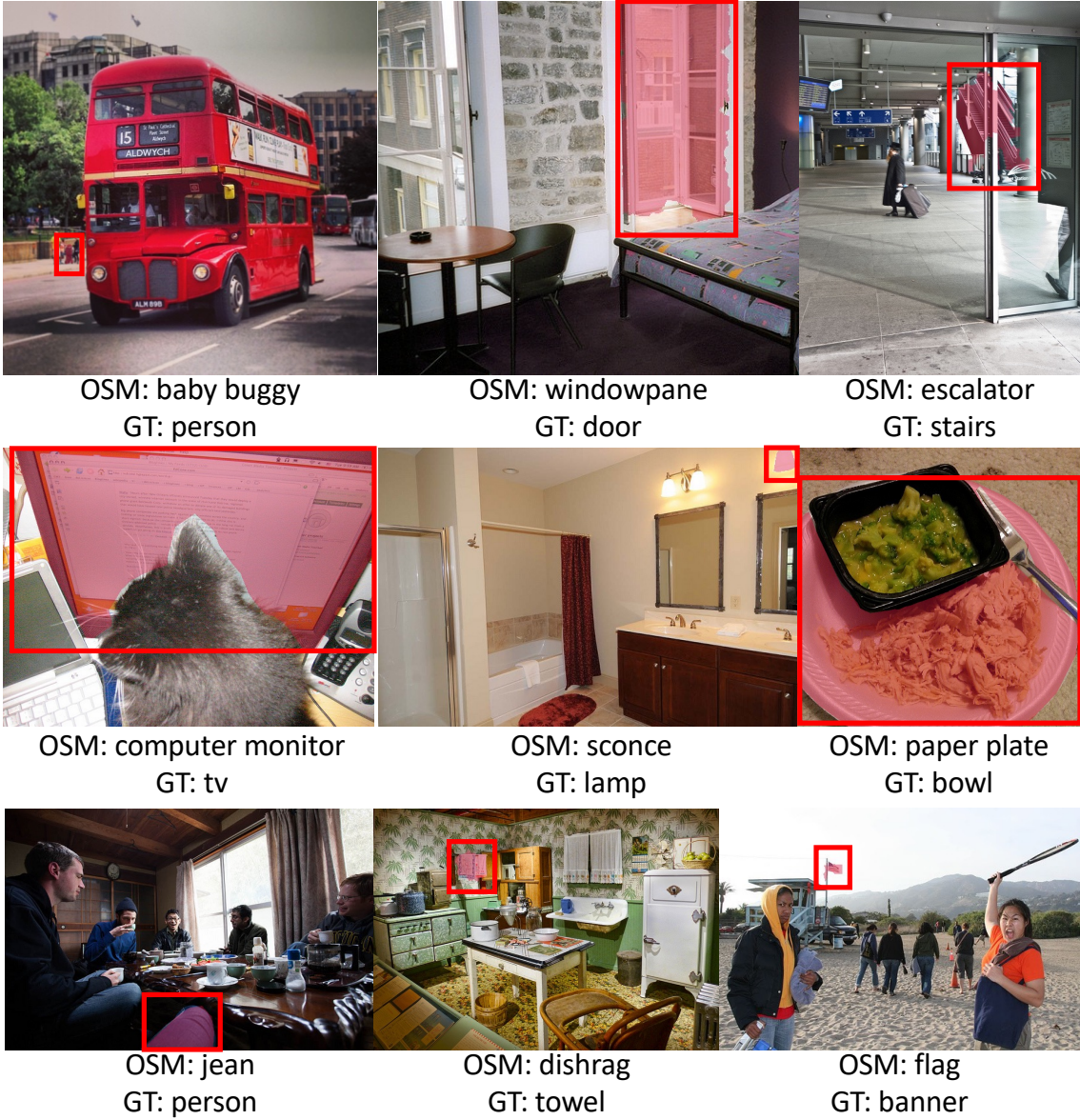


Figure 10. **Visualization of NIV cases on COCO val set using ground-truth mask.** We note that OSM can predict a more felicitous class compared to ground-truth, where annotations are limited to the fixed vocabulary and thus usually less expressive. We highlight the mask region with bounding box for better visualization purposes. Best viewed zoom in.



Figure 11. **Visualization of NIV cases on ADE20K val set using ground-truth mask.** We note that OSM can predict a more felicitous class compared to ground-truth, where annotations are limited to the fixed vocabulary and thus usually less expressive. We highlight the mask region with bounding box for better visualization purposes. Best viewed zoom in.